

IMECE2024-144980

ULTRASONIC VIBRATION-ASSISTED SCRATCHING PROCESS OF SAPPHIRE: EFFECTS OF FEEDING SPEED

Shah Rumman Ansary, Sarower Kabir, Weilong Cong

Department of Industrial, Manufacturing, and Systems Engineering, Texas Tech University
Lubbock, TX, USA

ABSTRACT

There is a recent surge in interest in sapphire due to its distinctive physical and chemical properties, coupled with widely recognized, highly productive, and economical crystal growth techniques. The low fracture toughness and high hardness value of sapphire makes it a very challenging material to be machined. Scratching test using a single diamond abrasive grain is a great way to understand the material removal mechanism and deformation characteristics of sapphire-like brittle materials. This test result can also be used to simulate and predict sapphire's cutting force and material removal mechanism during other multi-abrasive machining processes like grinding and lapping. Experimental investigations have shown that vertical ultrasonic vibration-assisted scratching can improve the cutting forces, scratch quality, and material removal characteristics of sapphire wafers compared to conventional scratching. However, the effect of different feeding speeds on the scratching process of sapphire wafers has not been studied yet. To address this research gap, this experimental study examines how both feeding speed and ultrasonic vibration impact vertical cutting force, scratch quality, and the material removal mechanism of sapphire wafers. We have tested four distinct feeding speeds, spanning from extremely slow (0.1 mm/s) to moderately fast (100 mm/s). We have analyzed the cutting force data and observed the scratch-induced microscopic features and thus got some insight into the deformation patterns attributed to the surface morphologies of sapphire. This experimental investigation validates that higher feeding speed with ultrasonic vibration can lead to better scratch quality with reduced microcrack formation.

1. INTRODUCTION

Sapphire, a monocrystalline form of α -alumina (Al_2O_3) is one of the hardest materials with a Mohs hardness of 9. It has several distinctive features, including high hardness, excellent thermal resilience, chemical resistance, good structural durability, high dielectric strength, effective light transmission, and relatively good lattice spacing. All these unique characteristics make sapphire a good substrate material to be used in the semiconductor industry. It is widely used in high-speed integrated circuit (IC) chips, as thin film substrates, as well as in abrasion-resistant windows for industrial and military purposes, and for the scratch-resistant crystal faces of wristwatches [1–5]. The development of Silicon-on-Sapphire (SoS) technology for high-frequency RF transceivers and switches was driven by the robust dielectric strength and favorable lattice compatibility between r-plane sapphire and silicon [6]. Sapphire can be used both as a passive substrate material and as an active device. By investigating intrinsic and impurity-related flaws in alumina, along with advancements in material engineering, highly efficient luminescent crystals with diverse applications have been developed. Examples of such crystals include Ruby (α -alumina:Cr) and Ti-Sapphire laser crystals [7,8]. Surface machining and micromachining is an integral part of sapphire wafer fabrication for all these applications. The surface quality and morphology of sapphire play a vital role in the functional performance of sapphire in applications. Sapphire, being a brittle material, is difficult to machine due to its low fracture toughness and high hardness value. Microcracking and edge chipping are also very common during fine surface machining of sapphire. Generally, the traditional machining process induces residual stress on the sapphire planar surface that impacts and degrades its mechanical and optical properties. Therefore, it is necessary to explore newer

Keywords: Ultrasonic vibration; Single diamond scratching; Feeding speed; Cutting force; Edge chipping.

techniques and novel mechanisms for surface machining of sapphire wafers.

In the last few decades, non-traditional machining (NTM) has been widely investigated for brittle materials such as silicon wafers, sapphire wafers, SiC wafers, GaN wafers [9–12]. NTM processes can be broadly classified into three categories: chemical NTM methods, thermal NTM methods, and mechanical NTM methods. Chemical wet etching and electrochemical machining fall into chemical NTM methods. While the chemical NTM methods offer the advantages of minimal microcracks and surface damage they have some significant drawbacks, including slow processing speed, difficult control mechanism, and very high chemical disposal costs. Thermal NTM methods are mostly different types of laser-based machining methods. Due to the high temperature rise around the laser scanning path, thermal NTM has the disadvantage of forming heat-affected zones (HAZ) and unwanted material oxidation. This HAZ compromises the strength of sapphire wafers and so its mechanical properties are degraded. Two types of mechanical NTM methods commonly employed are abrasive jet machining (AJM) and abrasive waterjet machining (AWJ) [13–15]. The common drawback for both AJM and AWJ is free abrasive particles that reduce the machining accuracy. Rotary ultrasonic machining (RUM), another mechanical NTM process, is considered as an effective and efficient machining process for hard-brittle materials. The concept of RUM was first proposed

in the 1960s but recently it has got more attention due to its excellent advantages with both conventional machining and micromachining.

Ultrasonic vibration has been found to be advantageous in different manufacturing processes. Ultrasonic vibration has a frequency greater than 20kHz. This high frequency is significantly greater than the natural frequency of any machine tools used in a manufacturing process. In RUM, the rotating tool is also vibrated with an ultrasonic frequency with very low amplitude (typically less than 5 μm) which facilitates the machining process. In RUM, the kinematic motion of the cutting tool is a combination of the rotational motion of the spindle, the vertical ultrasonic vibration of the piezoelectric transducer, and the horizontal feeding motion of the machine table [16]. RUM process requires a lower cutting force compared to traditional machining and it can generate better surface quality and morphology with fewer microcracks [17]. RUM process also has the advantages of higher machining speed and the capability of machining intricate and small features effectively compared with the chemical NTM methods [18]. Unlike the laser-based thermal NTM, RUM avoids the formation of HAZ, which could increase the strength of the semiconductor wafers [19]. Research on the RUM of ceramics and ceramic matrix composites has shown that it can effectively reduce both cutting force and edge chipping [20]. Because of all these advantages, RUM is also used widely for the machining process for sapphire materials.

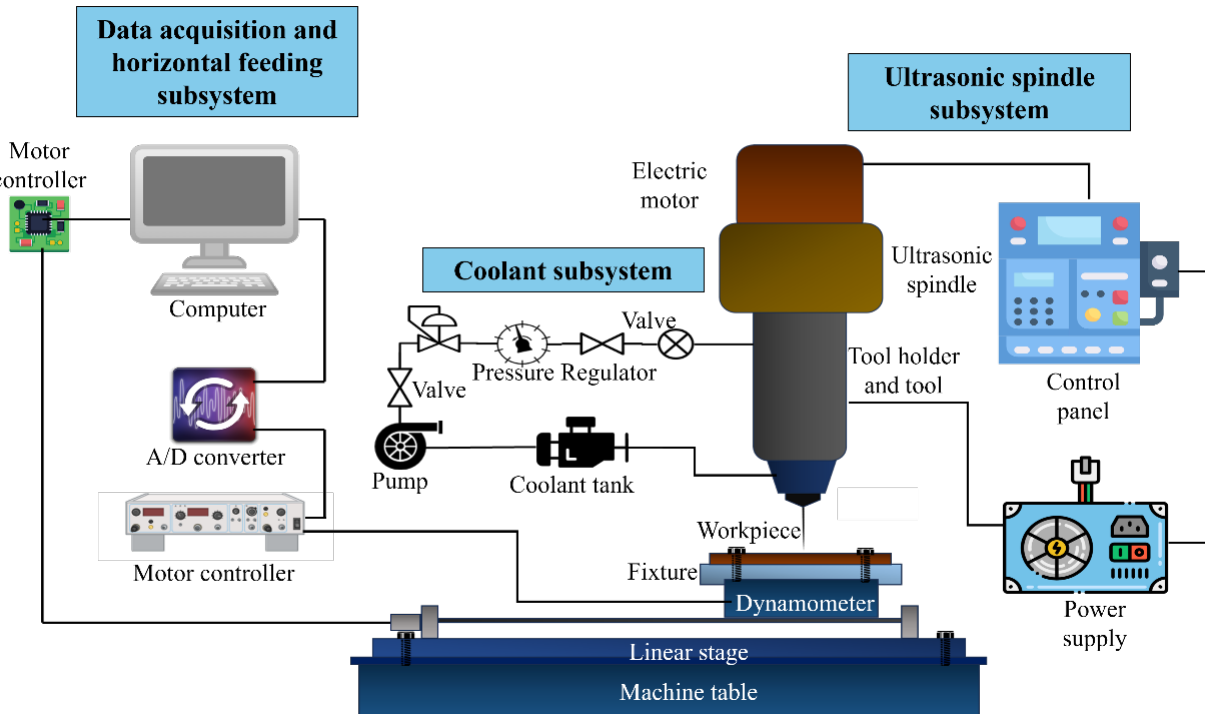


FIGURE 1: The illustration of the single diamond-scratching process of sapphire wafer.

Scratching test using a single diamond abrasive grain is generally conducted to investigate the scratch resistance and material removal mechanism of brittle materials like sapphire, silicon, SiC composites, etc [21]. The single-diamond scratching test result can be used to simulate and predict the cutting force and material removal mechanism of other multi-abrasive machining processes. Many researchers have reported single-diamond scratch studies on monocrystalline silicon wafers and sapphire wafers [11–15,22,23]. Yunze *et al.* showed that single-diamond scratching with ultrasonic vibration produces reduced cutting force both through experimental investigation and theoretical analysis [24]. Zhang *et al.* reported that ultrasonic vibration-assisted scratching of sapphire reduces the cutting force and largely improves the scratch quality with more plastic removal area [21]. However, in all those studies, the feeding or scratching speed was kept constant. So, we could not get any insight into the effect of the scratching speed in the sapphire wafer scratching process. Different feeding speeds in single-diamond scratching can be considered analogous to different tool rotation speeds for multi-abrasive cutting processes. So, to better understand the cutting force and material removal mechanism of multi-abrasive cutting processes under different tool rotation speeds, single-diamond scratching under different feeding speeds needs to be investigated. In this experimental investigation, we aimed to fill this knowledge gap by scratching sapphire wafers using a single diamond tool at four different speeds, such as 0.1 mm/s, 1 mm/s, 10 mm/s, and 100 mm/s under conditions with and without ultrasonic vibrations. A linear ramping indentation depth from 0 to 8 μm along the scratch length of 8 mm was obtained in both cases. The vertical cutting forces during these scratching tests were measured and optical microscopic (OM) images of the scratched grooves at different indentation depths were collected. Examining the results of the

cutting forces and observing the scratch-induced microscopic features, the effects of different feeding speeds on scratch quality under different indentation depths were analyzed and discussed.

2. EXPERIMENT PROCEDURES

2.1 Experimental Setup

The scratching test experiments, both conventional scratching (CS) and ultrasonic vibration-assisted scratching (UVAS) were conducted using a Sonic-Mill (series 10) rotary ultrasonic machine (Albuquerque, NM, USA). Figure 1 shows the experimental setup that has three subsystems: an ultrasonic spindle subsystem, a coolant subsystem, and a data acquisition and horizontal feeding subsystem. A controller and an ultrasonic generator were the two important parts of the ultrasonic spindle subsystem. The controller was employed to change the power of the ultrasonic vibration according to our design of experiments. The ultrasonic generator has piezoelectric transducers that produce vertical ultrasonic vibrations (20 kHz). This ultrasonic vibration is then mechanically transmitted to the cutting tool. The coolant subsystem had a pump and a coolant tank with coolant, specifically made to reduce the excess heat produced at the intersection of the cutting tool and ultrasonic generator. The horizontal feeding subsystem had a linear positioner (VS-15, Newmark, USA), a motion controller (model: NSC-A1, Newmark, USA), and the controller software (QuickMotion NSC-A1 v1.0.2, Newmark, USA). This horizontal feeding subsystem was used to ensure uniform and accurate horizontal feeding motions for both CS and UVAS experiments. With the help of QuickMotion software, we maintained different feeding speeds ranging from 0.1 mm/s to 100 mm/s. The data acquisition, measurement, and analysis will be discussed in the measurement procedure section.

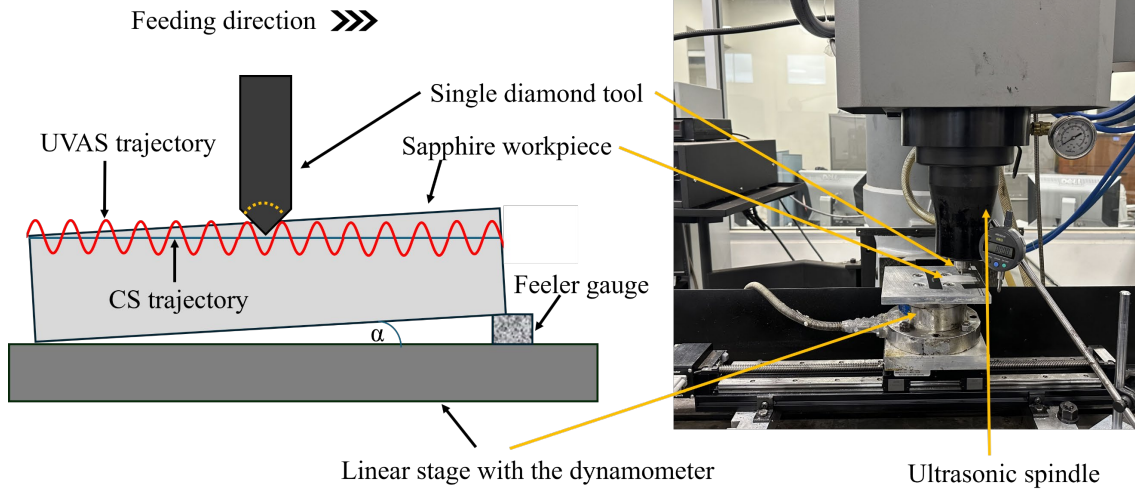


FIGURE 2: The illustration and photograph of the setup for the continuous increase of indentation depth.

Table 1

Properties of sapphire wafer workpiece

Properties	Unit	Values
Density at 20°C	kg/m ³	3.98
Mohs hardness		9
Knoop hardness		1500
Tensile strength	MPa	350
Flexural strength	MPa	600
Shear modulus	GPa	145
Poisson's ratio		0.29

2.2 Workpiece Material and Tool

The workpieces were single-side polished c-plane sapphire wafers (650 μm thickness, University Wafer, Inc., USA). The cutting or scratching tool was a single diamond dresser (Praztech, Switzerland) with a 90° included angle. Before the experiment, the sapphire wafers were cut into small pieces and cleaned using isopropyl alcohol (IPA) and deionized (DI) water. Then it was firmly fixed on the top of the dynamometer with adhesive tape. One end of the sapphire wafer was elevated by placing a 0.05 mm feeler gauge underneath to ensure a continuous increase of indentation depth along its length. Figure 2 shows the illustration and photograph of the tool and workpiece with the feeler gauge. A digital indicator (ID-S112, Mitutoyo Corp., Japan) was used to measure the height difference between the two ends of the sapphire wafer. Simple calculation from that

height difference and length of the sapphire workpiece gave us the value of the indentation depths at different scratching points. The digital indicator was also used to find the amplitude of the ultrasonic vibration. The properties of the sapphire wafer have been listed in Table 1.

2.3 Measurement Procedure

The vertical cutting forces were collected by the data acquisition subsystem. This subsystem consisted of a dynamometer (Type 9272, Kistler, Winterthur, Switzerland), a charge amplifier (Type 5070, Kistler, Winterthur, Switzerland), and DynoWare software (Kistler, Winterthur, Switzerland). The dynamometer was fixed onto the linear stage to capture the charge signals generated by the cutting forces in all three directions. These analog signals were then amplified by the charge amplifier and converted into digital signals by the A/D converter. The DynoWare software was used to collect the digital signals. An optical microscope (OM) (DSX-510, Olympus, Tokyo, Japan) was used to observe and measure the scratching features. In this study, we used Origin software (OriginLab, Massachusetts, USA) to plot and analyze the cutting forces. We used the Savitzky-Golay filter to smooth our measured cutting force data and took mean values of the cutting forces at different indentation depths. We also used ImageJ software to measure and analyze the OM images to calculate the edge chipping. Different input parameters and operational variables are listed in Table 2.

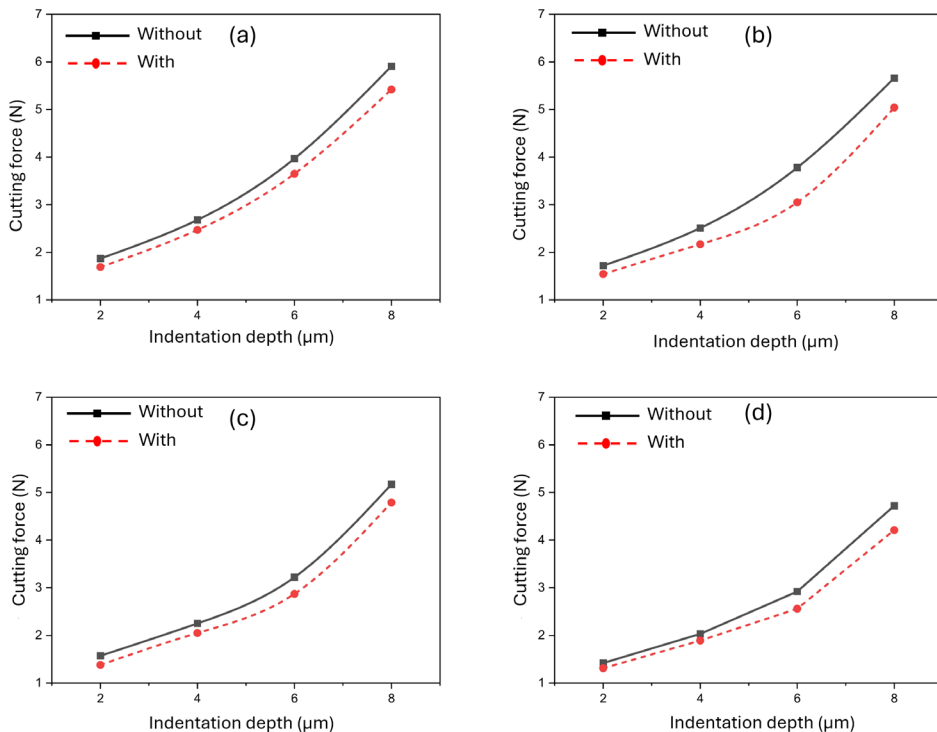


FIGURE 3: Change of vertical cutting force with indentation depth at (a) 0.1 mm/s feeding speed, (b) 1 mm feeding speed, (c) 10 mm feeding speed, (d) 100 mm feeding speed.

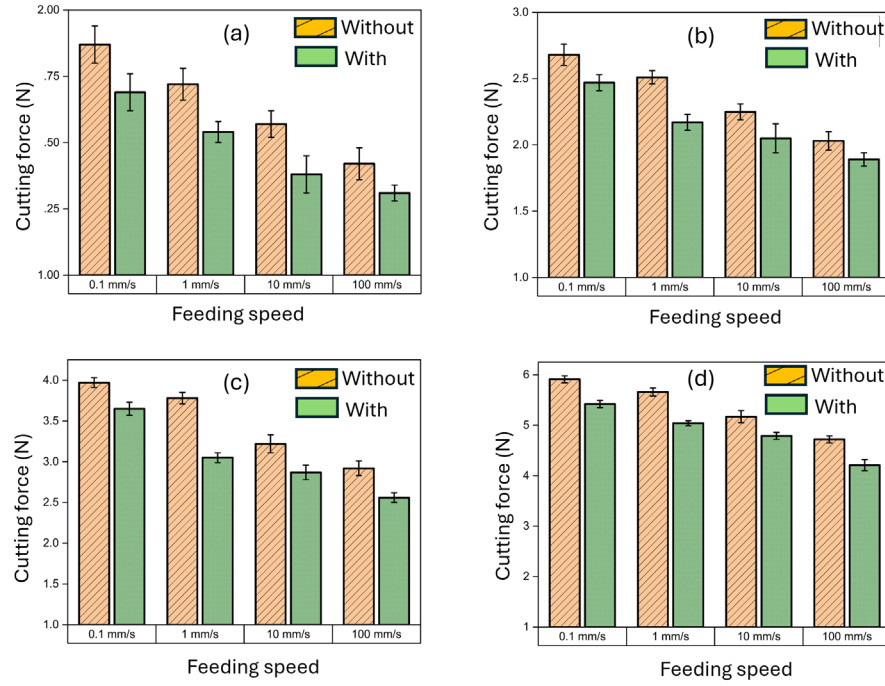


FIGURE 4: The average vertical cutting force values for different feeding speeds at (a) 2 μm indentation depth, (b) 4 μm indentation depth, (c) 6 μm indentation depth, (d) 8 μm indentation depth.

Table 2
Experimental conditions for the single-diamond scratching test

Input variables	Unit	Values
Feed rate	mm/s	0.1, 1, 10, 100
Ultrasonic power	%	40
Vertical ultrasonic amplitude	μm	3
Vertical ultrasonic frequency	kHz	20
Tool-tip angle	degree	90
Workpiece tilting angle, α	degree	0.057

3. RESULTS AND DISCUSSION

During the traditional CS process, the indentation depth increased gradually with the increase of scratching time due to the slope of the workpiece. The indentation depth in the CS process can be calculated from the scratch time or scratch length and the workpiece tilting angle. On the other hand, the actual indentation depth at a certain scratching length in the UVAS process would differ from that at that particular scratching length in the CS process for two reasons. Firstly, the actual indentation depth in the UVAS process would be periodically changed due to the ultrasonic frequency of the rotary ultrasonic machine. Secondly, as the ultrasonic amplitude (3 μm) was always associated with the UVAS process, the indentation depth for UVAS at a certain scratching length would be always significantly higher than the indentation depth for CS at that particular scratching length. In our experiment, we used only one cutting tool with a diamond tip of 90 degrees. The relationship

between groove width and indentation depth is shown in Equation 1:

$$\text{Groove width, } w = 2d \tan(45^\circ) \quad \dots(1)$$

Where d is the indentation depth. To be consistent with the scratches' cutting force and edge chipping result, the indentation depths for both CS and UVAS processes were kept the same by doing some calculations, analysis, and maneuvering. At first, the same groove widths for both processes were marked from the OM images. Then the indentation depths were calculated and the corresponding scratch lengths for the UVAS process were later determined. The cutting force and OM images were compared based on this corresponding scratching length. Table 3 shows the various scratching lengths and corresponding indentation depths and groove widths for the CS process.

Table 3

Scratching lengths and theoretical corresponding indentation depths and groove widths for the CS process

Scratching length (mm)	Indentation depth (μm)	Groove width (μm)
2	2	4
4	4	8
6	6	8
8	8	16

3.1 Effects of Feeding Speed on the Cutting Force

The vertical cutting forces at different indentation depths under the conditions with and without ultrasonic vibrations have been plotted in Figure 3. It shows that with the increase of indentation depth, the vertical cutting force is gradually increased for both CS and UVAS processes. This is because at higher indentation depth the groove width will be higher and thus the total material removal will be significantly higher. The exponential increasing curve of vertical cutting force indicates that with the increase of indentation depth as well as groove width, the material removal mechanism is gradually changed.

It is easily understood from all four plots of Figure 3 that, the UVAS process generates lower cutting force values than the CS process. For all four scratching speeds, the vertical cutting force generated in the UVAS process is about 10-15% lower than those generated in the CS process. It can prove that the periodic contact between the cutting tool and the sapphire workpiece due to ultrasonic vibration can effectively reduce the vertical cutting force for similar indentation depths. Similar phenomena were observed by other studies carried out on silicon substrates, SiC ceramics, and CFRP composites [16,20,25]. This result can be extended for multi-abrasive machining and thus we can infer that the use of ultrasonic vibration greatly influences reducing the vertical cutting force during any kind of machining process. The values of the scratching force with and without ultrasonic vibration are in good agreement with the values reported for the scratch tests performed on the c-plane sapphire block [23]. Figure 4 shows the average vertical cutting force values for different feeding speeds under the conditions with and without

ultrasonic vibration. From these plots, we can infer that at higher scratching speeds the vertical cutting force values drop significantly. At 2 μm indentation depth, the vertical cutting force for 0.1 mm/s feeding speed for the CS process was about 1.85 N. For a tenfold increase in feeding speed, that is, at 1 mm/s, that cutting force value becomes 1.7 N which is about 10% less. Similar results can be observed for 10 and 100 mm/s feeding speeds too. At 10 mm/s feeding speed, the vertical cutting force for the CS process is about 1.6 N, and at 100 mm/s feeding speed, the vertical cutting force for the CS process is about 1.4 N. A similar phenomenon is observed in the UVAS process. At the same indentation depth (2 μm), we observed a 1.65 N cutting force value for the UVAS process with 0.1 mm/s feeding speed. When the feeding speed is increased to 1 mm/s, that cutting force lowers down to about 1.5 N. At 10 and 100 mm/s feeding speeds, the cutting force becomes 1.35 N and 1.25 N respectively. This proves that the average vertical cutting force for both CS and UVAS processes can be significantly reduced if we set up the feeding speed at 100 mm/s or more. At low feeding speed, the contact between the diamond tool and the sapphire workpiece at a particular region persists for a long time which can generate localized crack generation and edge chipping and thus leads to higher cutting force. On the other hand, at a higher feeding speed, the diamond tool passes a particular region within a very short time and thus there is less chance of crack generation and as a result, it generates lower cutting force. However, due to the very short period of contact between the cutting tool and the sapphire wafer during high-speed scratching, there is greater chance of slipping and irregular scratching which has been discussed in the next section.

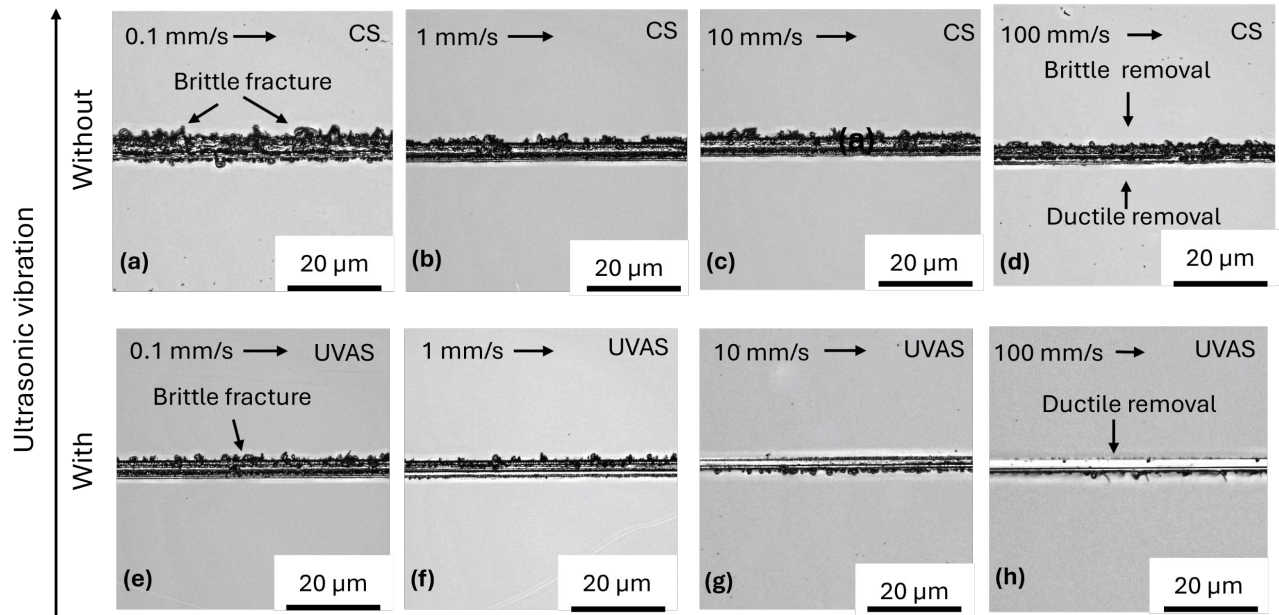


FIGURE 5: The morphologies of the scratch-induced features under different feeding speeds for the CS and UVAS process

3.2 Effects of Feeding Speed on the Scratch Quality and Material Removal Mechanism

Figure 5 shows the OM images of the scratch-induced features for both CS and UVAS processes at different feeding speeds. We took OM images and analyzed the surface morphologies at 2 μm , 4 μm , 6 μm , and 8 μm indentation depths. The OM images of Figure 5 are taken at 6 μm indentation depth and this typical case can be used to explain the material removal mechanism under different feeding speeds.

From figures 3 and 4, it is evident that with the increase of indentation depth, the cutting force is always increased. Higher vertical cutting force could increase the residual stress inside the sapphire workpiece, which resulted in the generation of microcracks and the removal of large chips. By analyzing the morphological changes of the scratch-induced features, the transition of ductile-brittle material removal can be determined. The smaller magnitude of cutting force indicates elastic-plastic deformation or ductile material removal. The larger value of cutting force implies brittle fracture and microcrack generation. From Figure 4(c), the average vertical cutting force for CS at 0.1 mm/s feeding speed is about 4 N while that for CS at 100 mm/s is 2.9 N. If we look at the corresponding surface morphology in Figure 5(a), we can find that CS at 0.1 mm/s has more cracks, and the scratched groove is primarily formed due to the brittle material removal of the sapphire workpiece. On the other hand, the surface morphology for CS at 100 mm/s in Figure 5(d) shows very minimal crack generation and the material removal is dominant by the elastic-plastic material removal from the

sapphire wafer. Similar phenomena is obtained for the UVAS process. From Figure 4(c), the average cutting force for UVAS at 0.1 mm/s feeding speed is 3.6 N, and that for UVAS at 100 mm/s feeding speed is 2.5 N. Corresponding surface morphologies in Figure 5(c) and 5(h) shows that there are brittle fractures at 0.1 mm/s feeding speed while there is no brittle fracture at 100 mm/s feeding speed. If we compare the surface and scratch quality between the CS and UVAS processes at the same feeding speed, fewer cracks and less brittle material removal are observed for the UVAS process.

This material removal mechanism and surface quality can also be explained in terms of edge-chipping data. Edge chipping is very common and cannot be avoided during the machining of brittle materials like sapphire wafers. However novel machining processes generally generate less edge chipping than regular machining processes. The edge chipping at different indentation depths for different feeding speeds has been shown in Figure 6. It shows that UVAS has lower edge chipping compared to the corresponding CS at the same feeding speed and the same indentation depth. Comparing the edge chipping values and the scratch-induced features, it can be inferred that UVAS helps suppress the occurrence of brittle material removal and thus improves the surface quality of the scratched region. So, combining these two result analyses, in general, it can be said that UVAS at higher feeding speeds generate smooth grooves primarily formed due to the ductile material removal of the workpiece.

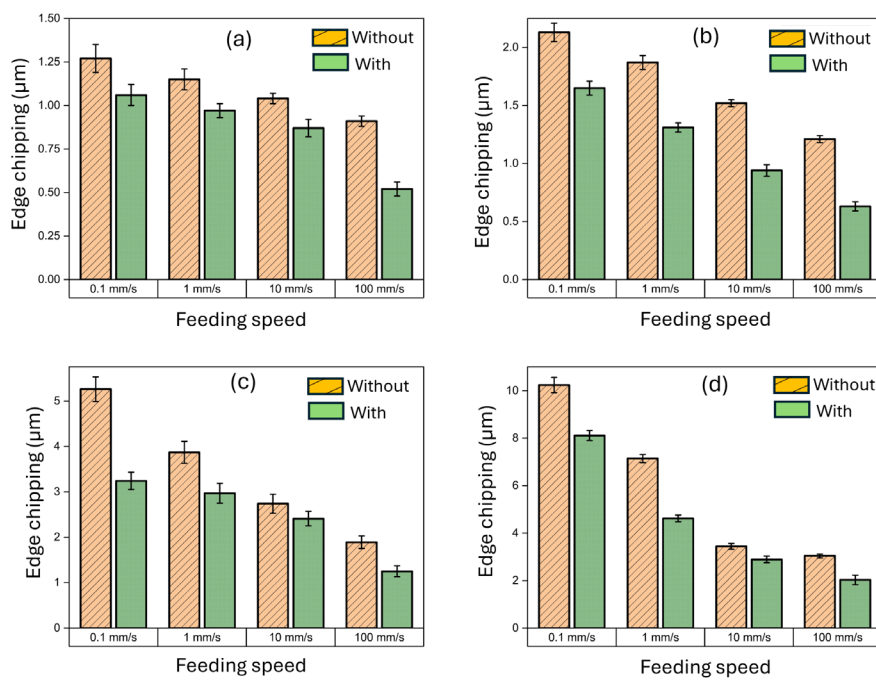


FIGURE 6: The average edge chipping values for different feeding speeds at (a) 2 μm indentation depth, (b) 4 μm indentation depth, (c) 6 μm indentation depth, (d) 8 μm indentation depth.

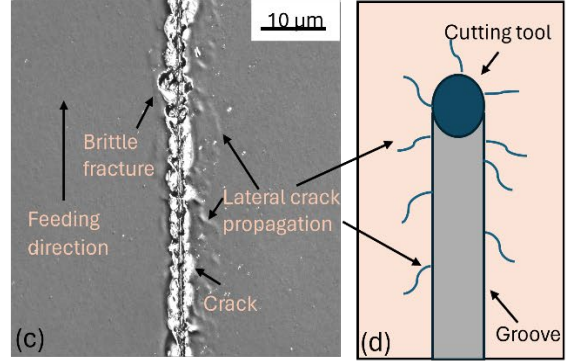
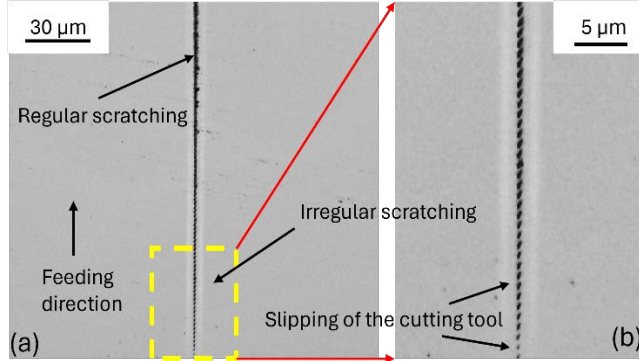


FIGURE 7: (a) Slipping at the onset of high-speed (100 mm/s) feeding for UVAS, (b) the zoomed view of slipping, (c) a picture of the crack generation and propagation at low speed (0.1 mm/s) feeding for CS, and (d) a schematic top view of the crack

However, higher feeding speeds have some drawbacks too. Very high feeding speeds have slipping issues at the onset of the scratch. Figure 7(a) and (b) can be used to explain this issue. As sapphire is a very hard material, it is difficult to machine and so the diamond cutting tool needs a reasonable amount of time to be in contact with the workpiece to make an indent. At very high speeds, there is not enough contact or processing time and as a result, slipping occurs with no indentation marks or some irregular indentations. This generally happens at the very beginning of the scratching test when the indentation depth is less than 2 μm . Gradually with the increase of the indentation depth this slipping issue disappears, and a regular indentation mark is seen. The slipping and irregular indentation marks have been found in both CS and UVAS at high feeding speeds of 100 mm/s. It can be presumed that, if we increase the feeding speed more, this issue may arise more frequently and so there should be a trade-off to avoid slipping.

Figures 7 (c) and (d) show the microcrack generation and propagation at higher indentation depths at low feeding speed for the CS process. The low feeding speed has a higher contact or processing time and thus there is more possibility of large part removal and edge chipping caused by the brittle material removal. Lateral crack propagation indicates that there is residual stress inside the workpiece and that might lead to median crack propagation too.

4. CONCLUSION

In this study, single-diamond scratching tests have been conducted on the sapphire wafer under different feeding or scratching speeds. Both traditional CS and UVAS processes have been compared here. The major limitation of this experimental investigation is that very high speed (greater than 100 mm/s) has not been tested here. The linear positioner used in this experiment has a maximum feeding speed of 100 mm/s. In the future, the experimental setup will be improved to further study the contribution of very high-speed scratching and also the effects of different level of power. The key findings of this study are:

1. In both CS and UVAS processes, with the gradual increase of indentation depth as well as groove width, the cutting force in the vertical direction was increased owing to the higher material removal from the workpiece.

2. The UVAS process generates about 10-15% less cutting force than the CS process at different feeding speeds. This proves that the periodic contact between the cutting tool and the sapphire workpiece in the UVAS process facilitates the scratching and thus produces a lower cutting force.

3. For both CS and UVAS processes, a higher feeding speed generates a lower cutting force. The long process time at lower feeding speed is prone to brittle material removal and thus produces higher cutting force.

4. The scratch quality at higher feeding speed is much better compared to that at low feeding speed. At higher feeding speeds, the material removal is primarily dominated by elastic-plastic material removal. 10 mm/s and 100 mm/s feeding forces generate smooth scratches which is mostly due to the ductile removal of the sapphire material from the groove. In contrast, the material removal at lower feeding speed is primarily dominated by the brittle fracture, mostly at higher indentation depths. The longer process time leads to large part removal, higher edge chipping, and brittle fracture. Also, there is a greater chance of microcrack generation and propagation at lower feeding speeds.

5. The drawback of very high feeding speed is slipping and uneven scratching at lower indentation depths. This happens because of the sapphire's high hardness and the inadequate duration of contact between the diamond tool and the sapphire wafer workpiece to initiate an indentation.

ACKNOWLEDGEMENTS

This work was supported by the U.S. National Science Foundation through the award CMMI- 2102181.

REFERENCES

[1] Akselrod, M. S., and Bruni, F. J., 2012, "Modern Trends in Crystal Growth and New Applications of Sapphire," *J. Cryst. Growth*, **360**, pp. 134–145.

[2] Khattak, C. P., Guggenheim, P. J., and Schmid, F., 2003, "Growth of 15-Inch Diameter Sapphire Boules," R.W. Tustison, ed., p. 47.

[3] Wang, A., Gollapudi, S., May, R. G., Murphy, K. A., and Claus, R. O., 1995, "Sapphire Optical Fiber-Based Interferometer for High Temperature Environmental Applications," *Smart Mater. Struct.*, **4**(2), pp. 147–151.

[4] Nakamura, S., 1998, "The Roles of Structural Imperfections in InGaN-Based Blue Light-Emitting Diodes and Laser Diodes," *Science* (80-), **281**(5379), pp. 956–961.

[5] Xiao, H., Deng, J., Pickrell, G., May, R., and Wang, A., 2003, "Single-Crystal Sapphire Fiber-Based Strain Sensor for High-Temperature Applications," *Light. Technol. J.*, **21**, pp. 2276–2283.

[6] Culurciello, E., 2009, *Silicon-on-Sapphire Circuits and Systems*, McGraw-Hill, Inc.

[7] Maiman, T. H., 1960, "Stimulated Optical Radiation in Ruby," *Nature*, **187**(4736), pp. 493–494.

[8] Moulton, P. F., 1986, "Spectroscopic and Laser Characteristics of Ti: Al₂O₃," *JOSA B*, **3**(1), pp. 125–133.

[9] Pal, P., and Sato, K., 2015, "A Comprehensive Review on Convex and Concave Corners in Silicon Bulk Micromachining Based on Anisotropic Wet Chemical Etching," *Micro Nano Syst. Lett.*, **3**, pp. 1–42.

[10] Reynaerts, D., Meeusen, W., and Van Brussel, H., 1998, "Machining of Three-Dimensional Microstructures in Silicon by Electro-Discharge Machining," *Sensors Actuators A Phys.*, **67**(1–3), pp. 159–165.

[11] Singh, M., Singh, S., and Kumar, S., 2020, "Experimental Investigation for Generation of Micro-Holes on Silicon Wafer Using Electrochemical Discharge Machining Process," *Silicon*, **12**, pp. 1683–1689.

[12] Wang, H.-J., and Yang, T., 2021, "A Review on Laser Drilling and Cutting of Silicon," *J. Eur. Ceram. Soc.*, **41**(10), pp. 4997–5015.

[13] Melentiev, R., and Fang, F., 2018, "Recent Advances and Challenges of Abrasive Jet Machining," *CIRP J. Manuf. Sci. Technol.*, **22**, pp. 1–20.

[14] Park, D.-S., Cho, M.-W., Lee, H., and Cho, W.-S., 2004, "Micro-Grooving of Glass Using Micro-Abrasive Jet Machining," *J. Mater. Process. Technol.*, **146**(2), pp. 234–240.

[15] Haghbin, N., Spelt, J. K., and Papini, M., 2015, "Abrasive Waterjet Micro-Machining of Channels in Metals: Comparison between Machining in Air and Submerged in Water," *Int. J. Mach. tools Manuf.*, **88**, pp. 108–117.

[16] Wang, H., Pei, Z. J., and Cong, W., 2020, "A Mechanistic Cutting Force Model Based on Ductile and Brittle Fracture Material Removal Modes for Edge Surface Grinding of CFRP Composites Using Rotary Ultrasonic Machining," *Int. J. Mech. Sci.*, **176**, p. 105551.

[17] Ya, G., Qin, H., Yang, S., and Xu, Y., 2002, "Analysis of the Rotary Ultrasonic Machining Mechanism," *J. Mater. Process. Technol.*, **129**(1–3), pp. 182–185.

[18] Yamada, K., Yamada, M., Maki, H., and Itoh, K. M., 2018, "Fabrication of Arrays of Tapered Silicon Micro-/Nano-Pillars by Metal-Assisted Chemical Etching and Anisotropic Wet Etching," *Nanotechnology*, **29**(28), p. 28LT01.

[19] Luft, A., Franz, U., Emsermann, L., and Kaspar, J., 1996, "A Study of Thermal and Mechanical Effects on Materials Induced by Pulsed Laser Drilling," *Appl. Phys. A Mater. Sci. Process.*, **63**(2), pp. 93–101.

[20] Jin, J., Wang, X., Bie, W., Chen, F., and Zhao, B., 2024, "Machinability of SiCf/SiC Ceramic Matrix Composites Using Longitudinal-Torsional Coupled Rotary Ultrasonic Machining," *Int. J. Adv. Manuf. Technol.*, **131**(5–6), pp. 2465–2476.

[21] Zhang, C., Feng, P., and Zhang, J., 2013, "Ultrasonic Vibration-Assisted Scratch-Induced Characteristics of C-Plane Sapphire with a Spherical Indenter," *Int. J. Mach. Tools Manuf.*, **64**, pp. 38–48.

[22] Amer, M. S., El-Ashry, M. A., Dosser, L. R., Hix, K. E., Maguire, J. F., and Irwin, B., 2005, "Femtosecond versus Nanosecond Laser Machining: Comparison of Induced Stresses and Structural Changes in Silicon Wafers," *Appl. Surf. Sci.*, **242**(1–2), pp. 162–167.

[23] Liang, Z., Wang, X., Wu, Y., Xie, L., Jiao, L., and Zhao, W., 2013, "Experimental Study on Brittle–Ductile Transition in Elliptical Ultrasonic Assisted Grinding (EUAG) of Monocrystal Sapphire Using Single Diamond Abrasive Grain," *Int. J. Mach. Tools Manuf.*, **71**, pp. 41–51.

[24] Li, Y., Zhang, D., Wang, H., Ye, G., He, R., and Cong, W., 2022, "Theoretical and Experimental Investigations on Rotary Ultrasonic Surface Micro-Machining of Brittle Materials," *Ultrason. Sonochem.*, **89**, p. 106162.

[25] Ning, F., Cong, W., Wang, H., Hu, Y., Hu, Z., and Pei, Z., 2017, "Surface Grinding of CFRP Composites with Rotary Ultrasonic Machining: A Mechanistic Model on Cutting Force in the Feed Direction," *Int. J. Adv. Manuf. Technol.*, **92**(1–4), pp. 1217–1229.